Surface Science 604 (2010) 2098–2105

Contents lists available at ScienceDirect

Surface Science

journal homepage: www.elsevier.com/ locate/susc

Thermodynamics and kinetics of CO and benzene adsorption on Pt(111) studied with pulsed molecular beams and microcalorimetry

Alexander Schießer *, Peter Hörtz, Rolf Schäfer

Eduard-Zintl-Institut für Anorganische und Physikalische Chemie, Technische Universität Darmstadt, Petersenstraße 20, 64287 Darmstadt, Germany

ARTICLE INFO

Article history:
Received 15 April 2010
Accepted 1 September 2010
Available online 8 September 2010

Keywords:
Microcalorimetry
Sticking probability
Adsorption energies
Carbon monoxide
Benzene
Pt(111)

ABSTRACT

The adsorption and desorption of the system CO/Pt(111) and C_6H_6/Pt(111) at 300 K has been investigated with a pulsed molecular beam method in combination with a microcalorimeter. For benzene the sticking probability has been measured in dependence of the coverage θ. For coverages $\theta>0.8$ transient adsorption is observed. From an analysis of the time-dependence of the molecular beam pulses the rate constant for desorption is determined to be 5.6 s^{-1}. With a precursor-mediated kinetic adsorption model this allows to obtain also the hopping rate constant of 95.5 s^{-1}. The measured adsorption enthalpies could be best described by $(199-77\theta-51\theta^2)$ kJ/mol, in good agreement with the literature values. For CO on Pt(111) also transient adsorption has been observed for $\theta>0.95$ at 300 K. The kinetic analysis yields rate constants for desorption and hopping of 20 s^{-1} and 51 s^{-1}, respectively. The heats of adsorption show a linear dependence on coverage $(131-38\theta)$ kJ/mol between $0\leq\theta\leq0.3$, which is consistent with the desorption data from the literature. For higher coverage (up to $\theta=0.9$ML) a slope of −63 kJ/mol describes the decrease of the differential heat of adsorption best. This result is only compatible with desorption experiments, if the pre-exponential factor decreases strongly at higher coverage. We found good agreement with recent quantum chemical calculations made for ($\theta=0.5$ML).

1. Introduction

Modification of surfaces and interfaces, and therewith the control of their physico-chemical properties is of fundamental interest for various disciplines. This endeavor might be more fruitful, if simple systems like single crystal surfaces are understood at first. For example regarding the Haber–Bosch process, the rate limiting step in the heterogeneously catalyzed chemical reaction to ammonia is the adsorption of nitrogen on Fe(100) [1,2]. Therefore, the experimentally determined heat of adsorption is an informative value when comparing different catalyst surfaces, and a key property to discuss the microscopic processes involved in heterogenous catalysis [2–4].

Different methods have been developed to measure the adsorption enthalpy. In the past decades often temperature-programmed techniques have been deployed, giving rise to a desorption of the adsorbate, which itself is followed by mass spectrometry [2,5–9]. Subsequently modeling the desorption kinetics facilitates extracting the activation energy of the desorption process. In the case of a vanishing energy barrier the heat of adsorption can be calculated from this experimental data as well. Wherever the adsorbate cannot be desorbed intact upon heating, or where the desorption models and their involved presumptions are undesired, a direct method for the measurement of adsorption enthalpies is necessary [3,4,10,11]. Early attempts of determining adsorption heats on single crystals directly with calorimetry were made by Kyser and Masel [12] and Kovar et al. [13]. However, the first single crystal adsorption calorimeter (SCAC) giving data for various systems was pioneered by King et al. [3]. In their setup a pulsed molecular beam was used in combination with a mercury–cadmium–telluride detector to measure adsorption enthalpies of gaseous compounds on various single crystal surfaces [3]. C. T. Campbell and coworkers improved the sensitivity of the SCAC by using a pyroelectric polyvinylidene fluoride (PVDF) foil in mechanical contact with a thin substrate to study adsorption of low vapor pressure molecules [4,10,11,14]. We also developed an adsorption microcalorimeter combined with a pulsed molecular beam source, which allows one to study the adsorption thermodynamics and desorption kinetics of both high and low vapor pressure molecules. Within this article results are presented for CO and benzene on Pt (111). The Pt(111) surface was chosen because recent calorimetric data are already available for benzene adsorption, which enables us to validate the functioning of our setup [10]. For the adsorption of CO on Pt(111) only an older set of calorimetric data exists, which shows some discrepancies to thermal desorption experiments and recent quantum chemical calculations [15,16]. Therefore, we have reinvestigated the adsorption enthaplies for CO on Pt(111) with an independent setup in order to contribute new calorimetric results to the discussion.

* Corresponding author.
E-mail address: schiesser@cluster.pc.chemie.tu-darmstadt.de (A. Schießer).

0039-6028/$ – see front matter © 2010 Elsevier B.V. All rights reserved.
doi:10.1016/j.susc.2010.09.001

2. Experimental

The experiments were performed in two stainless steel ultrahigh vacuum (UHV) chambers, separated by a gate valve and with base pressures $<5\cdot10^{-10}$mbar. The sample preparation chamber was equipped with a turbo molecular pump (pumping speed 170 Ls^{-1}), an Argon sputter gun, a radiative heater (250 W-filament) and a low energy electron diffraction optics (MiniLEED from OCI). The SCAC chamber with a volume of about 15 L is pumped by a turbo molecular pump (pumping speed 450 Ls^{-1}) and is equipped with the calorimeter, a pulsed molecular beam source and a quadrupole mass spectrometer (QMS 112 from Balzers), that is placed neither in the line of sight of the source nor of the sample.

2.1. Sample preparation

A 2 μm thick Pt(111) single crystal (Mateck) was sandwiched between two 100 μm Ta sheets (12×12 mm), each had a 7 mm diam. hole in the center. After spot welding them, the obtained sandwich was mounted on a sample holder, containing an 8 mm diam. hole, in order to provide access to the back side of the sample. Then the sample was cleaned by Ar sputtering (750 V, 5 μA/cm^2) and annealing in $5\cdot10^{-7}$ mbar O_2 at 850 K by radiative heating with the tungsten filament located 4 mm from the back side of the Pt(111). The temperature of the sample during annealing was measured using an infrared sensor. Sputtering and annealing cycles followed by flash annealing to 1000 K were repeated until the single crystal revealed good LEED patterns. X-ray Photoelectron Spectroscopy (XPS) was used to confirm cleanness of the sample and impurities were below its detection limit. The cleaned sample was transferred from the preparation chamber into the SCAC chamber to reach room temperature.

2.2. Molecular beam source

The piezoelectric pulsed molecular beam source [17], which permits us to investigate both low and high vapor pressure molecules, is the main difference compared to the SCAC setup deployed in Campbell's group [18], and is described briefly here. A piezoelectric disk translator, driven by a high voltage pulse, opens a nozzle which allows the molecules of the vapor phase to escape from the gas reservoir, thereby forming a pulsed molecular beam, which enters the sample in the SCAC chamber. From the pressure decrease in the gas reservoir after several pulses one can easily calculate the number of molecules per pulse by applying the ideal gas law. In the present experiments the reservoir contains about 1 mbar of either anhydrous benzene (99.8% purity) or CO (99.97% purity). The anhydrous benzene was used without any additional cleaning step, due to the low solubility of atmospheric gases in benzene [19]. The beam source was operated with pulses of 50 ms duration and a repetition rate of 0.5 Hz. The pressure peaks of the molecular beam pulses were typically $3\cdot10^{-8}$mbar.

The fraction of the molecular beam intercepted by the sample as a function of the distance between the nozzle of the gas doser and the sample is displayed in Fig. 1. By using the initial sticking probability $s_0=0.96\pm0.01$ of benzene on Pt(111) reported in the literature [18], the fraction f of benzene was determined. We decided to perform our experiments at a working distance of $L=8$ mm, corresponding to a fraction of $f=0.31\pm0.01$, in order to avoid gradients across the sample, which might adulterate the measurement of the heat of adsorption. The variation of the intercepting fraction versus nozzle-to-sample distance for CO is similar to the data of benzene, when using the initial sticking probability of $s_0=0.84\pm0.01$ (see Section 3.2.1). Therefore we conclude that the beam profile of the gas doser is not influenced by the mass of the molecules in a significant way.

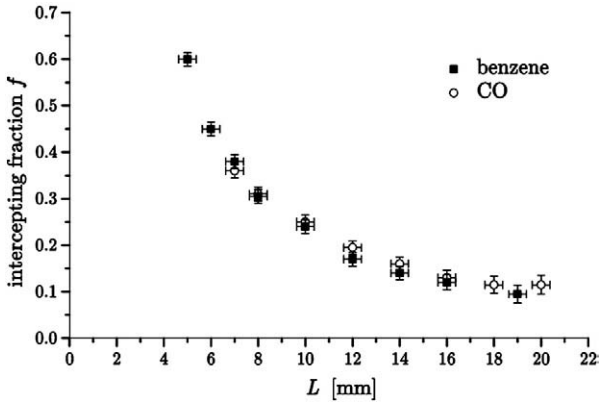

Fig. 1. The fraction of the molecular beam intercepted by the sample f as a function of nozzle-to-sample distance L. The squares represent the data obtained for benzene (using an initial sticking probability of 0.96 ± 0.01 [18]) and the circles for CO (using an initial sticking probability of $s_0=0.84\pm0.01$ (see 3.2.1).

2.3. Measurement of heats of adsorption

In Fig. 2 a schematic setup of the SCAC is presented.

The calorimeter design follows that of Campbell's group [14]. To be more specific, it consists of a 9 μm thick pyroelectric polymer ribbon (β-polyvinylidene difluoride, PVDF) (6 mm×25 mm) with gold electrodes on both sides for electric contact. This ribbon is clamped (together with a 25 μm Kapton foil to provide a better mechanical stiffness) between copper blocks to build an arc. The PVDF/Kapton arc is gently pressed to the back side of the cleaned Pt(111) to guarantee thermal contact.

At a distance of 6 mm from the source a gold plated orifice disk (2 mm thick) and a gold flag, which covers the orifice (7 mm diam. hole) are mounted. Together with the calorimeter the sample was driven in contact with the orifice (flag closed) and the pulsed molecular beam source was switched on.

All molecules coming from the source were scattered by the flag or the orifice disk, and thus could not reach the Pt(111). After a few pulses the flag was opened and the molecules could impinge onto the Pt(111) surface. The orifice disk provided that only molecules heading for the Pt(111) were able to pass — undesired adsorption on other parts was avoided.

The adsorption of molecules caused an increase of the temperature of the Pt(111) surface and also of the pyroelectric PVDF foil. The pyroelectric current was amplified with a current-to-voltage converter by a factor of 10^{11} V/A. After the adsorption process was finished, the gold flag was closed again to prove the stability of the molecular

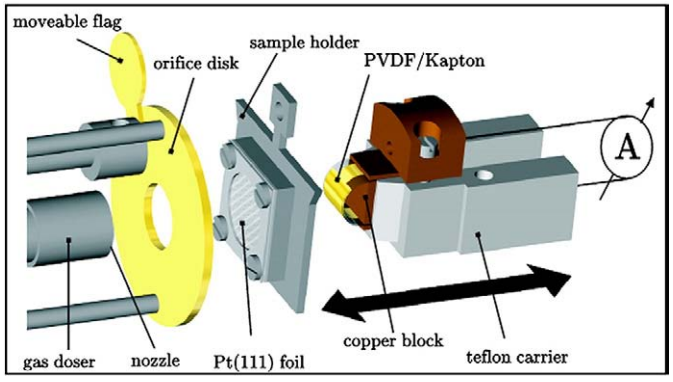

Fig. 2. Schematic setup of the SCAC experiment: To start a calorimetric measurement the teflon carrier is moved towards the sample holder until mechanical contact is obtained. Then the combined sample holder/teflon carrier setup is driven close to the orifice disk.

beam source. During each SCAC experiment the pyroelectric signal, the signal from the pressure decrease in the reservoir of the pulsed molecular beam source, as well as the signal of the quadrupole mass spectrometer (QMS) were collected synchronously with two USB6008 (from National Instruments) data acquisition units.

Before and after such a calorimetric measurement, calibration of the microcalorimeter was carried out with laser pulses striking the front side of the single crystal surface through a view port. Generation of the laser pulses (50 ms length) of known energy was achieved with a diode laser (645 nm), a tailor made laser shutter [20] and a NIST certified photo diode. Furthermore, for the calculation of the absorbed laser energy, the reflectivity of the Pt(111) foil and losses due to absorption of the view port had to be taken into account. The reflectivity of 0.74 ± 0.01 at 645 nm was determined, using a NIST certified photodiode with a large surface area to collect all reflected light.

Measuring the current directly with a current-to-voltage converter has the advantage that the electric capacity of the detector does not influence the pyroelectric signal. The pyroelectric current is known to be proportional to the variation of temperature with time and thus the integrated pyroelectric signal represents the actual temperature (or the pyroelectric generated electric charge) with respect to the initial temperature of the PVDF foil. In Fig. 3 the pyroelectric current (a) and the integrated signal (b) are displayed for three situations: a laser pulse strikes the Pt(111) sample, only adsorption of CO occurs and desorption of CO occurs after adsorption took place. All three curves exhibit a nearly indistinguishable behavior for the first 50 ms after the corresponding pulse was applied, but then the desorption process leads to a significant mismatch. Therefore we evaluate the peak of the pyroelectric current, in order to get the information about the heat released during adsorption, without taking the slower desorption process into account.

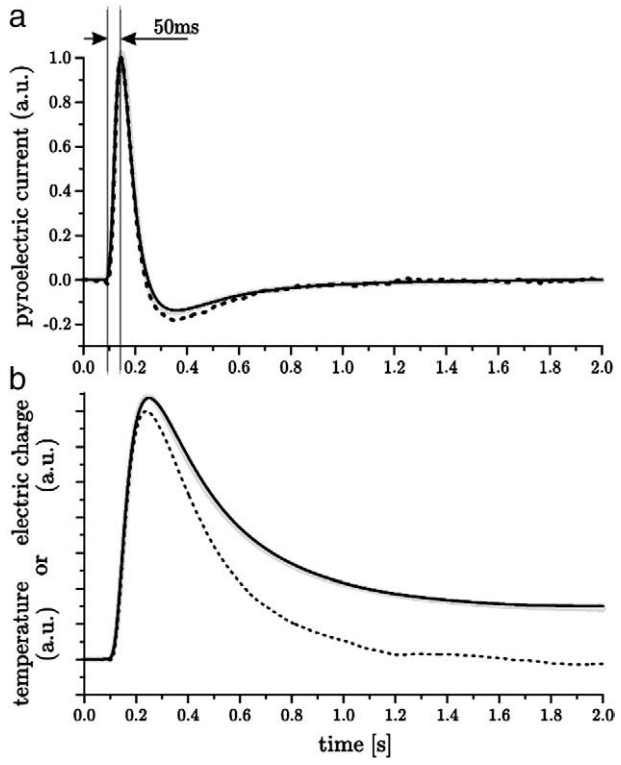

Fig. 3. a.) Averaged and normalized (to their peak) pyroelectric currents obtained with a 50 ms laser pulse (thick gray line), adsorption without desorption (thin black line), and adsorption with desorption taking place between the molecular pulses (dotted line). b.) Signals obtained by integration of the pyroelectric current, which correspond to the electric charge or the temperature respectively.

The pyroelectric peak current was proved being proportional to the absorbed laser energy between 0 and 50 μJ. The calorimeter constant of the presented experiments was 115 ± 15 nj/pA, depending on the quality of the contact and age of the pyroelectric ribbon. The pulse-to-pulse standard deviation of the measured heats of adsorption is about 10–15 nJ, similar to the accuracy reported recently in the literature, although our single crystal was twice as thick [4]. It might be worth mentioning, that we observed negative interfering signals when the PVDF foil was not supported by a Kapton foil. We suspect the change in the surface stress caused by adsorbing molecules, which is registered by the piezoelectricity of the PVDF foil, but is damped by the use of the Kapton foil.

3. Results and discussion

3.1. Benzene

3.1.1. Net sticking probability

Typical QMS data collected during an SCAC experiment for benzene on Pt(111) are shown in Fig. 4a. After the gold flag was opened, the QMS peaks were diminished due to the adsorption of benzene. Following a period of constant adsorption, the QMS peaks increased and start to saturate. According to the method originally developed by King and Wells [21] the *net sticking probability* is calculated from the total area $\int p_i dt$ under the QMS signal for each pulse i

$$s_{i,net} = \frac{1}{f}\left(1 - \frac{\int p_i dt}{\int p_0 dt}\right), \tag{1}$$

wherein $\int p_0 dt$ corresponds to the area under the peak of the QMS signal for pulses with the flag closed. The normalized areas under the QMS signal are shown in Fig. 4b. From this it becomes clear that the net adsorption terminates about 25–30 pulses after opening the flag. The fraction of impinging molecules intercepted by the crystal surface f was determined to be 0.31 ± 0.01, as described before.

Defining a monolayer as the saturation coverage at 300 K, a monolayer is reached as soon as the net sticking probability attains zero. Considering the number of molecules per pulse (determined from the pressure decrease in the reservoir of the pulsed molecular

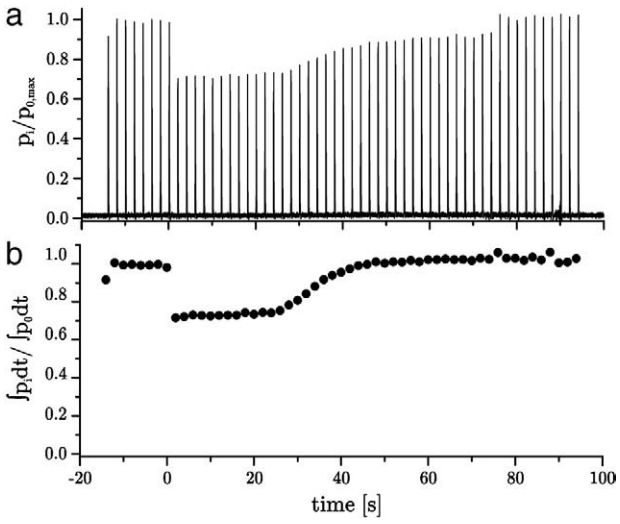

Fig. 4. a.) Normalized QMS signal (78 amu) for the adsorption of benzene on Pt(111) at 300 K. After eight pulses (each containing $1.8 \cdot 10^{13}$ benzene molecules) the flag was opened, after 37 pulses the flag was closed again. b.) The circles refer to the normalized area under the QMS signal for each pulse.

beam source) permits one to obtain $N_{i,net}^{ads}$, i.e. the net number of adsorbed molecules per pulse

$$N_{i,net}^{ads} = N_{pulse} \cdot f \cdot s_{i,net}. \tag{2}$$

Summation of overall pulses reveals that for a monolayer $8.4 \cdot 10^{13}$ molecules are adsorbed on the Pt(111) surface on an area of 0.38 cm^2 at 300 K. This is in good accordance with the literature value of a monolayer $2.3 \cdot 10^{14}/cm^2$ [10]. Thus the total coverage after each pulse i is given by

$$\theta_i = \frac{\sum_{i=1}^{i} N_{i,net}^{ads}}{\sum_{i=1}^{i=\infty} N_{i,net}^{ads}} = \frac{\sum_{i=1}^{i} s_{i,net}}{\sum_{i=1}^{i=\infty} s_{i,net}}. \tag{3}$$

The coverage dependence of the net sticking probability is displayed in Fig. 5.

The coverage dependence of the sticking probability on flat metal surfaces is often described by a precursor-mediated behavior. Kisliuk [22] introduced a model in which he considered that a molecule either strikes an occupied site, where it might desorb with a certain probability or it hops to a neighboring site. If this new site is empty, the molecule can either chemisorb or desorb. The sticking probability s is expressed in dependence of the coverage θ and the initial sticking probability s_o.

$$s = \frac{s_o}{1 + K\left(\frac{\theta}{1-\theta}\right)}, \text{ with } K = \frac{k_d}{k_d + k_h}. \tag{4}$$

The Kisliuk parameter K contains the desorption and hopping rate, k_d and k_h respectively. Therefore the parameter describes the degree of mobility of the precursor state: small positive values of K correspond to a highly mobile precursor, whereas $K \rightarrow 1$ describes an immobile precursor and hence a simple Langmuir kinetics. It should be mentioned, that this model neglects adsorbate interactions other than site blocking and ad-layer ordering.

Using Eq. (4) to fit the coverage dependence of the net sticking probability, as shown in Fig. 5, an initial sticking probability of $s_o = 0.96 \pm 0.01$ and a Kisliuk parameter of $K = 0.06 \pm 0.01$ is found which is in reasonable agreement with the value of 0.035 reported by Campbell et al. [10].

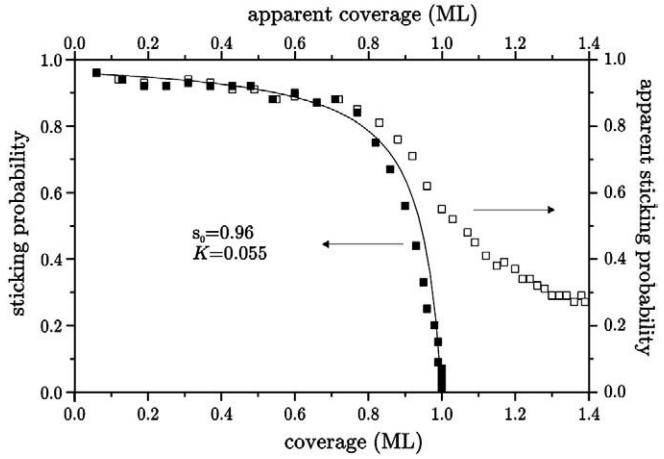

Fig. 5. Coverage dependence of the apparent (□) and net sticking (■) probability for benzene on clean Pt(111) at T = 300 K obtained from Fig. 4. A model for precursor-mediated adsorption is fitted to the data using the Kisliuk Eq. (4) (solid curve). One monolayer (ML) corresponds to $2.3 \cdot 10^{14}$ molecules/cm^2.

3.1.2. Desorption kinetics at θ>0.8

With pulsed experiments desorption between the pulses could be observed from a comparison of the peak maxima with respect to the area under the QMS signals. While the area under the QMS signal for each pulse includes the non sticking molecules plus the molecules eventually desorbed between the pulses, the height $p_{i,max}$ of the QMS signals only contains the molecules that never stuck on the single crystal surface. In order to take also the transiently adsorbed molecules into account, a so-called *apparent sticking probability* is introduced, which is given in analogy to Eq. (1) for each pulse by

$$s_{i,app} = \frac{1}{f}\left(1 - \frac{p_{i,\max}}{p_{0,\max}}\right), \tag{5}$$

but now the peak heights have to be used for the calculation of $s_{i,app}$. We took the QMS peak heights which were reached within about 50 ms after the beginning of the gas pulse, because after this time no more new molecules enter the chamber. As the QMS signal is the result of a square like pulse from the gas doser folded with an exponential function arising from the pumping speed, integration up to the pulse-on-time would lead to the same result. Therefore the apparent sticking probability we are using is an equivalent expression to the "short-time sticking probability" used by Lytken et al. [23].

With the number of apparently adsorbed molecules per pulse $N_{i,app}^{ads}$ the apparent coverage could be determined in the same way as the net coverage was calculated. Since the apparent sticking probability takes also the transiently adsorbed molecules into account, the apparent coverage just appears to be greater than unity, because desorption between the pulses is not considered. The apparent sticking probability is displayed as a function of their coverage in Fig. 5. It is obvious that the net and the apparent sticking probability show the same behavior for a coverage between $\theta = 0$ and 0.8, but then the net sticking probability tends to zero, while the apparent sticking probability remains finite and tends towards a constant value, i.e. at $\theta > 0.8$ a part of the benzene molecules is transiently adsorbed and become desorbed in the period of 2 s between the gas pulses.

In order to learn more about this desorption process a simple kinetic model of consecutive elementary steps is used. Let us consider that a molecular gas pulse was applied and that the number of intermediately, transiently adsorbed molecules A_{ads} is given by $N_{ads}(0)$. These molecules leave the surface with a desorption rate constant $k_d = 1/\tau_d$, i.e. the transiently adsorbed molecules can be found in the gas phase after they persisted on the surface with a residence time of τ_d. The desorbed molecules A_g stay for a certain time τ_p in the gas phase before they exit the vacuum chamber through the turbo molecular pump. Therefore τ_p is inverse to the pumping rate constant $k_p = 1/\tau_p$.

The kinetic model with the consecutive reaction steps is therefore described by

$$A_{ads} \xrightarrow{k_d} A_g \xrightarrow{k_p} A_{pump}. \tag{6}$$

Furthermore, one has to take into account, that there are still molecules in the gas phase which never stuck to the surface. The number of these molecules amounts to $N_g(0)$. Hence the total number of molecules in the gas phase N_g, which is measured directly with the QMS, is given by

$$N_g(t) = \left(N_g(0) + \frac{k_d}{k_p - k_d} N_{ads}(0)\right) \cdot e^{-t/\tau_p} + \frac{k_d}{k_p - k_d} N_{ads}(0) \cdot e^{-t/\tau_d}. \tag{7}$$

If the flag is closed, neither permanent nor transient adsorption takes place, thus Eq. (7) reduces to

$$N'_g(t) = N_g(0)' \cdot e^{-t/\tau_p}. \tag{8}$$

Fitting this function to the tail of a QMS signal with the gold flag closed yields $\tau_p = 36\,\text{ms}$, or $k_p = 28\,\text{s}^{-1}$ respectively.

In Fig. 6 two QMS signals are displayed, a QMS peak resulting from a molecular gas pulse with closed flag (dashed line) and another QMS peak at a net coverage of $\theta \approx 1$ (solid line). Obviously the peak with the closed flag is higher in magnitude but declines faster than the one with the open flag, because no transient adsorption followed by desorption takes place. However, the area (from 0 to 2 s) under both peaks is equal as can be seen from Fig. 4. In order to illustrate the different behavior of the two QMS signals the difference between them is shown in the inset of Fig. 6. The desorption rate constant is obtained by adjusting $N_g(t) - N'_g(t)$ with the help of Eqs. (7) and (8) to the measured data (dashed line in Fig. 6), revealing a residence time of $\tau_d = 180 \pm 20\,\text{ms}$, i.e. $k_d = 5.6\,\text{s}^{-1}$ at saturation coverage.

Now with the just obtained value for k_d and $K = 0.055$ and using Eq. (4) we are able to evaluate the hopping rate constant $k_h = 95.5\ \text{s}^{-1}$. Beside k_h the Gibbs energy of activation for the desorption process $\Delta^{\ddagger}G = \ln(k_d/\upsilon)RT$ may be estimated from the obtained k_d and a pre-exponential factor using the transition state theory of $\upsilon = kT/h = 6.25 \cdot 10^{12}\,\text{s}^{-1}$, yielding a value of 67 kJ/mol. This value is slightly smaller than the observed desorption energy of 70–69 kJ/mol by Ihm et al. [10].

3.1.3. Microcalorimetry

Typical pyroelectric data collected during an SCAC experiment for benzene on Pt(111) are shown in Fig. 7. The peak heights of the pyroelectric current are proportional to the heat released during adsorption. They are decreasing nearly in a linear way for the first 13 benzene pulses even if a constant sticking probability was observed. Then the pyroelectric signals decrease faster before they reach a constant value. The differential molar heats of adsorption $q_{cal,i}$ are calculated by dividing the heat released during the adsorption process by the mole number of apparently adsorbed molecules $N^{ads}_{i,app}$. The apparent number of adsorbed moles is used, because the height of the detected heat signals is only due to benzene adsorption. However, the differential molar heats for each pulse $q_{cal,i}$ have to be assigned to the coverage θ_i arising from the net sticking probability.

In a last step the increased kinetic energy of the benzene molecules in the thermal molecular beam has to be considered. Thus the observed

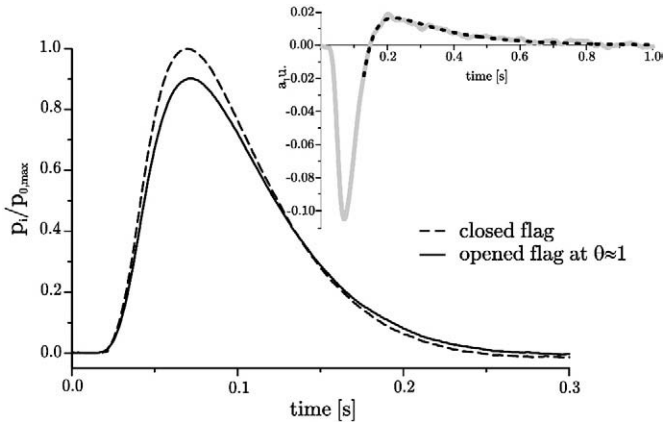

Fig. 6. Transient adsorption behavior at $\theta \approx 1$. Averaged QMS peaks with closed flag (dashed line) and open flag at $\theta \approx 1$ (solid line). The difference (grey line) between these two QMS peaks is shown in the inset. The dotted line is the fit taking Eqs. (7) and (8) into account.

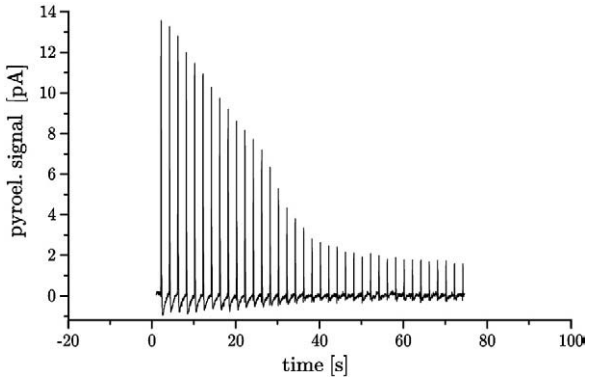

Fig. 7. Pyroelectric signals for the adsorption of benzene on Pt(111) recorded together with the QMS data depicted in Fig. 4.

heats $q_{cal,i}$ have to be corrected in order to obtain the differential molar adsorption enthalpies

$$q_{ads,i} = \Delta H_{ads,i} = -\left(q_{cal,i} + \frac{1}{2}RT\right). \tag{9}$$

Those are shown in Fig. 8 (filled squares) together with the integral heats of adsorption

$$\Delta H_{ads,integ} = \frac{\sum_1^i \Delta H_{ads,i} \cdot \Delta\theta_i}{\sum_1^i \Delta\theta_i}. \tag{10}$$

which are displayed as a thin solid line.

The measured coverage dependent differential heat of adsorption decreases from 200 kJ/mol ($\theta = 0$) to 72 kJ/mol ($\theta \approx 1$). The coverage dependence could be described best by $(199 - 77\theta - 51\theta^2)$ kJ/mol. The data are in nearly perfect agreement with the measurements of Ihm et al. [10] despite the slightly lower values for a coverage ranging between $\theta = 0.3$ and $\theta = 0.6$. The relative error is estimated to be 5 kJ/mol and the absolute error is about 4% due to the uncertainty in optical reflectivity of the sample and 2.5% due to the error in the determination of N_{pulse}. We stress out that the adsorption enthalpy is independent from the fraction f (and its error).

3.2. CO

3.2.1. Sticking probability

Typical data collected during an SCAC experiment for CO on Pt (111) are shown in Fig. 9. After opening the flag the QMS peaks were

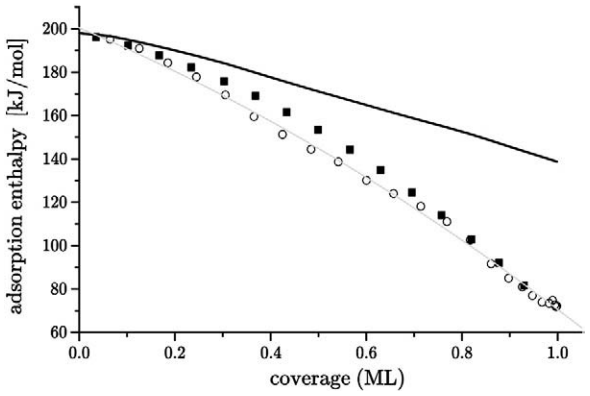

Fig. 8. Average of three measurements (○) of the differential molar adsorption enthalpies compared with the data of Campbell (■); solid line: integrated molar adsorption enthalpies. The grey solid line is a quadratic fit to our data.

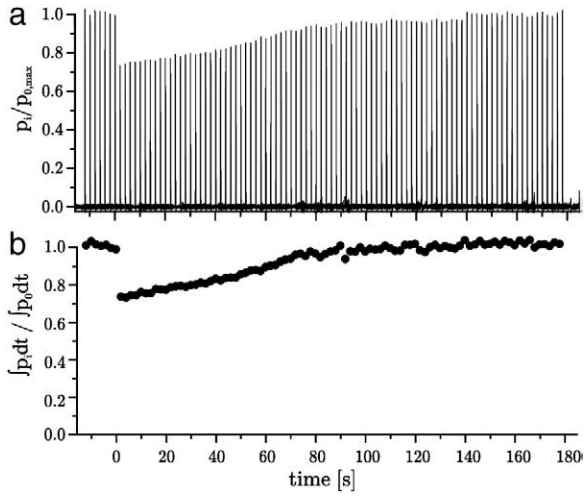

Fig. 9. a.)Normalized QMS signals (28 amu) for the adsorption of CO on Pt(111) at 300 K. After seven pulses (each contains $4 \cdot 10^{13}$ CO molecules) the flag was opened, after 68 pulses the flag was closed again. b.)The circles refer to the normalized area under the QMS signal for each pulse.

steadily recovering but did not reach the original peak height with the flag closed again.

In analogy to benzene the net sticking probability was calculated with Eq. (1) using the same fraction of $f=0.31$. The coverage was determined with Eq. (3) yielding a saturation coverage of $(7.5\pm0.1)\cdot 10^{14}$molecules/cm^2 at 300 K, a value that is within the experimental error in agreement with the literature [7,8,24]. In our definition this equals a monolayer. It should be noted that in the literature a monolayer is often defined as one adsorbate molecule per substrate atom. Within this definition a monolayer corresponds to $1.505\cdot 10^{15}$molecules/cm^2 [7], which is almost exactly twice the number of adsorbed molecules per cm^2 at the saturation coverage at 300 K. The coverage dependence of the net sticking probabilities is plotted in Fig. 10. Applying again the Kisluik model to the CO data an initial sticking probability of $s_0=0.84\pm0.01$ and $K=0.28\pm0.01$ has been found. Both values agree very well with those reported in the literature for 300 K, with s_0 ranging from 0.80 to 0.85 [3,5,8,25] and K ranging from 0.26 [24] to 0.30 [8].

The apparent sticking probability and the associated apparent coverage for 300 K are also plotted in Fig. 10. It is obvious that the net and the apparent sticking probability demonstrate the same behavior for a coverage ranging from $\theta=0$ to 0.95, but then the net sticking probability drifts to zero, while the apparent sticking probability remains finite and tends towards a constant value. This observation at

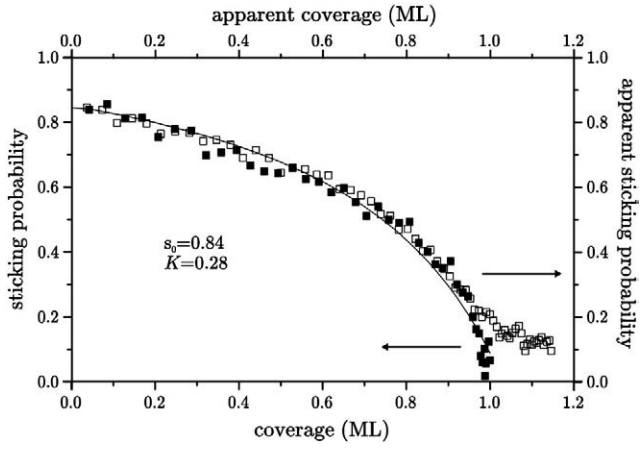

Fig. 10. Coverage dependence of the apparent (□) and net sticking (■) probability measured for CO on clean Pt(111) at T=300 K from Fig. 9. Best fit to the net sticking probabilities using the Kisliuk Eq. (4) (solid curve).

$\theta>0.95$ can be ascribed to CO molecules transiently adsorbed and which desorb in the period of 2 s between the gas pulses.

3.2.2. Microcalorimetry

Typical pyroelectric data collected during an SCAC experiment for CO on Pt(111) are shown in Fig. 11. The peak heights, respectively the released heat, are decreasing in a nearly linear way for the first 25 CO pulses, then the pyroelectric signals decrease more slowly until a steady state is reached.

In analogy to benzene the differential molar adsorption heats q_{cal} have been calculated from the heat released during each pulse and the mole number of adsorbed molecules. The differential and integrated molar adsorption enthalpies are shown in Fig. 12. The relative and absolute error is the same as for benzene on Pt(111).

Furthermore the differential adsorption enthalpy can be roughly described by a linear decay from initially 131 kJ/mol to 80 kJ/mol at $\theta=0.9$, then followed by a rapid decrease to 45 kJ/mol at the saturation coverage ($\theta\approx1$).

For the initial heat of adsorption values of typically 124 kJ/mol to 146 kJ/mol were derived from desorption experiments as reported in the literature [6–9,26,27], which are in reasonable agreement with the calorimetric data indicating the absence of an additional energy barrier for desorption. From another SCAC experiment the value found by Brown et al. [3] is somewhat higher (187 ± 11 kJ/mol) [3].

At 300 K for low coverage almost all CO molecules occupy on-top sites of the Pt(111) surface. For a coverage of $\theta=0.5$ still about 80% of the CO was found on-top and only 20% is bridged-bonded [26]. Consequently when comparing our values to the quantum chemical calculation done at $\theta=0.5$ the theoretically determined values for the on-top adsorption enthalpies (and also bridged, if they are available) have to be considered. In this comparison the measured differential heats of adsorption have to be integrated from zero up to 0.5 ML first. Our SCAC result and values from the theory are shown in Table 1.

A clear trend in the improvement of the theoretical calculations over the last few years becomes evident. The older calculations were performed with the Perdew–Wang-91-functional (PW91) (or the even older P86 and P88 respectively), whereas the newer investigations deployed the revised Perdew–Burke–Ernzerhof functionals (RPBE) [31]. The most recent quantum chemical calculation of Abild-Pedersen and Andersson [16] is in nearly perfect agreement with the experimental value even if the calculation refers to a temperature of 0 K.

Besides the initial or the adsorption enthalpy at a certain coverage the dependence of the adsorption enthalpies on coverage is more relevant. A linear decrease with a slope of $-38(\pm3)$ kJ/mol/ML (for $0<\theta<0.3$) of the differential heats of adsorption can be fitted to our SCAC data. This value is within the experimental errors in good agreement with the ones obtained by different desorption experiments as shown in

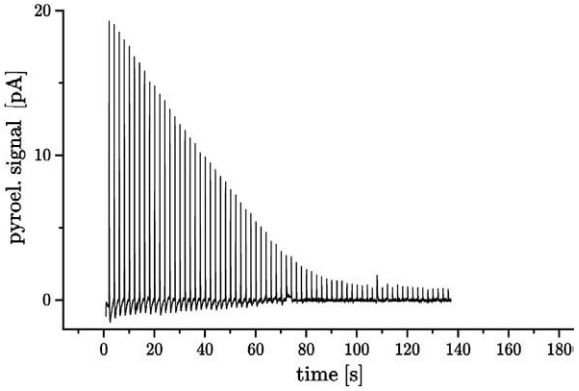

Fig. 11. Pyroelectric signals for CO adsorption on Pt(111), recorded together with the QMS data, depicted in Fig. 9.

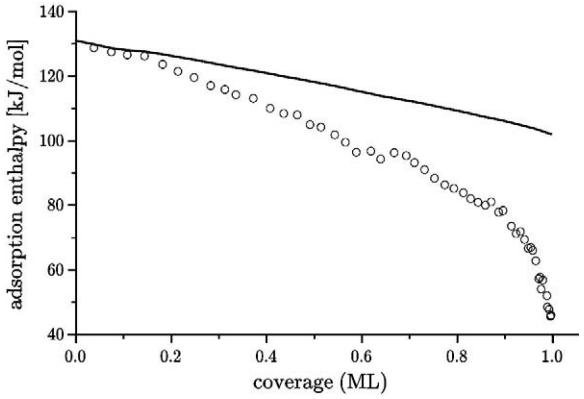

Fig. 12. Coverage dependent adsorption enthalpies for CO on Pt(111) at 300 K: average of four measurements for the differential heat of adsorption (○), the integral heat of adsorption (black solid line).

Table 1
Comparison of theoretical and the experimentally measured integral heats of adsorption at $\theta = 0.5$.

ΔH_{ads}	DFT method	Ref.
180 kJ/mol	PW91	Lynch et al. [28]
153 kJ/mol	B88 + P86	Zhang et al. [29]
150 kJ/mol	LDA + PW91	Bleakley et al. [30]
129 kJ/mol	RPBE	Gajdoš et al. [15]
117 kJ/mol	RPBE	Abild-Pedersen et al. [16]
117 kJ/mol	Experimental	This work

Table 2. The slopes obtained from desorption experiments using a kinetic first order models with a fixed pre-exponential factor υ are denoted with a star. These values are in less congruence with the SCAC data at high coverage, as our slope of the differential adsorption enthalpy becomes steeper with increasing coverage.

Because isotherms obtained by Kelemen et al. [6] suggested that the order of the desorption process decreased at coverages higher than $\theta = 0.45$ and became even negative near $\theta = 1$, they questioned the use of a first order process with a constant pre-exponential factor. In fact Taylor and Weinberg [33] pointed out that the so-called order plot [32] they were using did not consider that the pre-exponential factor might be a function of coverage. In other words, at higher coverage it is not the order of the desorption process that is changing, but rather the pre-exponential factor υ. Indeed their adsorption enthalpies are in good agreement within the range between $\theta = 0$ and 0.45 but differ at higher coverage due to the fixed pre-exponential factor. Moreover Seebauer et al. [5] were able to extract the coverage dependence of $\upsilon(\theta)$ from their data, starting at $10^{14.4 \pm 0.5}$ s^{-1} and dropping down to about $10^{7.5}$ s^{-1} at the saturation coverage. They did not use a desorption model but applied the Clausius–Clapeyron equation to their laser induced desorption measurement. Their coverage dependence of the differential heat of adsorption exhibits a slope of -67 ± 6 kJ/mol in the range of $\theta = 0$–0.9 which is comparable to our SCAC data.

We extracted a pre-exponential factor from the desorption behavior of CO on Pt(111) at the saturation coverage with the help of our kinetic model Eqs. (7) and (8) in analogy to benzene. The obtained residence time τ_d for transiently trapped CO molecules was 50 ± 20 ms, i.e. $k_d = 20$ s, and allows us to determine the hopping rate constant $k_h = 51$ s^{-1} with Eq. (4). Furthermore assuming the non-existence of an additional activation barrier the desorption energy is obtained from $E_d + RT/2 = \Delta H_{ads} = 45$ kJ/mol and applying the Arrhenius equation a pre-exponential factor of $\upsilon = 2 \cdot 10^9$ s^{-1} can be determined. Moreover this value points to a constrained transition state and is much smaller than the pre-exponential factors used for the evaluation of the TDS spectra.

4. Conclusion

We investigated the adsorption and desorption behavior of benzene and CO on Pt(111) using a new pulsed molecular beam source capable to dose both high and low vapor pressure molecules, and a modified detection mode of the pyroelectric microcalorimeter. With this setup we find good congruence with the coverage dependency of the sticking probability and adsorption enthalpies published by Campbell's group for the adsorption of benzene on Pt (111). Additionally the desorption energies of the transiently adsorbed benzene on Pt(111) obtained with our kinetic model at saturation coverage are in good agreement with their published data.

Reinvestigation of the system CO/Pt(111) confirmed an initial sticking probability of 0.84 and the precursor-mediated behavior which can be described by the Kisliuk model.

Further the initial adsorption enthalpy and its coverage dependency up to $\theta = 0.3$ agree well with the result of desorption experiments. For higher coverage the only agreement found is with the desorption data, where no fixed pre-exponential factor was used. Therefore the deviations between our SCAC data and the analysis of the TDS spectra seem to be mainly due to the coverage dependence of the pre-exponential factor. In addition our desorption analysis of transiently adsorbed CO at saturation coverage seem to confirm a constrained transition state. Recent quantum chemical calculations are in perfect agreement with our SCAC data.

Limitations of the experimental setup can be found, where the vapor pressure of the molecules is too low (<0.1 mbar at 300 K), or the sticking probability is very small. The first difficulty can be overcome by modification of the gas doser to work at elevated temperatures. The second problem can be solved by carrying out SCAC experiments at lower temperatures like already performed by Lytken et al. [4].

Table 2
Comparison of the coverage dependent differential adsorption enthalpies with desorption experiments.

$\Delta H_{ads}(\theta = 0)$	Slope [kJ/mol]	Range of θ	Method of determination	Ref.
133 kJ/mol	−29(±10)	0–0.26	He scattering^{*,a}	Poelsema et al. [27]
133 kJ/mol	−39(±8)	0–0.3	TDS^{*,f}	Kelemen et al. [6]
135 kJ/mol	−48(±6)	0–0.45	TDS^{*,f}	Kelemen et al. [6]
137 kJ/mol	−36(±8)	0–0.54	TDS^{*,r,j}	Campbell et al. [8]
135 kJ/mol	−35(±5)	0–0.4	Laser induced thermal desorption^{r,c}	Seebauer et al. [5]
141 kJ/mol	−65(±5)	0–0.9	Laser induced thermal desorption^{r,c}	Seebauer et al. [5]
138 kJ/mol	−32(±9)	0–0.6	Time-resolved isothermal desorption^{*,w}	Kinne et al. [26]
137 kJ/mol	−27	0–0.9	TDS^{*,r,i}	Ertl et al. [7]
124 kJ/mol	−27	0–0.9	TDS^{*,r,i}	McCabe and Schmidt [9]
131 kJ/mol	−38(±3)	0–0.3	SCAC	This work
132 kJ/mol	−52(±2)	0–0.45	SCAC	This work
138 kJ/mol	−63(±2)	0–0.9	SCAC	This work

*First order kinetics with a constant pre-exponential factor $^{j}\upsilon = 4 \cdot 10^{15} s^{-1}$ $^{i}\upsilon = 1 \cdot 10^{15} s^{-1}$ ^{w}Wigner-Polanyi-equation ^{a}Arrhenius plot ^{r}Redhead analysis ^{c}Clausius-Clapeyron equation and ^{f}Falconer and Madix [32].

Beyond that, measuring at lower temperature would additionally give an access to the adsorption entropy.

Acknowledgement

The authors acknowledge the work done by the mechanical and electronic workshop of our department.

References

[1] G. Ertl, Angew. Chem. Int. Ed. 47 (19) (2008) 3524.
[2] G. Ertl, S.B. Lee, M. Weiss, Surf. Sci. 114 (2–3) (1982) 527.
[3] W.A. Brown, R. Kose, D.A. King, Chem. Rev. 98 (2) (1998) 797.
[4] O. Lytken, W. Lew, C.T. Campbell, Chem. Soc. Rev. 37 (10) (2008) 2172.
[5] E.G. Seebauer, A.C.F. Kong, L.D. Schmidt, Surf. Sci. 176 (1–2) (1986) 134.
[6] S.R. Kelemen, T.E. Fischer, J.A. Schwarz, Surf. Sci. 81 (2) (1979) 440.
[7] G. Ertl, M. Neumann, K.M. Streit, Surf. Sci. 64 (2) (1977) 393.
[8] C.T. Campbell, G. Ertl, H. Kuipers, J. Segner, Surf. Sci. 107 (1) (1981) 207.
[9] R.W. McCabe, L.D. Schmidt, Surf. Sci. 66 (1) (1977) 101.
[10] H. Ihm, H.M. Ajo, J.M. Gottfried, P. Bera, C.T. Campbell, J. Phys. Chem. B 108 (38) (2004) 14627.
[11] J.M. Gottfried, E.K. Vestergaard, P. Bera, C.T. Campbell, J. Phys. Chem. B 110 (35) (2006) 17539.
[12] D.A. Kyser, R.I. Masel, Rev. Sci. Instrum. 58 (11) (1987) 2141.
[13] M. Kovar, L. Dvorak, S. Černý, Appl. Surf. Sci. 74 (1994) 51.
[14] J.T. Stuckless, N.A. Frei, C.T. Campbell, Rev. Sci. Instrum. 69 (6) (1998) 2427.
[15] M. Gajdoš, A. Eichler, J. Hafner, J. Phys. Condens. Matter 16 (8) (2004) 1141.
[16] F. Abild-Pedersen, M.P. Andersson, Surf. Sci. 601 (7) (2007) 1747.
[17] A. Schiesser, R. Schafer, Rev. Sci. Instrum. 80 (8) (2009) 086103.
[18] H.M. Ajo, H. Ihm, D.E. Moilanen, C.T. Campbell, Rev. Sci. Instrum. 75 (11) (2004) 4471.
[19] F.D. Evans, R. Battino, J. Chem. Thermodyn. 3 (6) (1971) 753.
[20] L.P. Maguire, S. Szilagyi, R.E. Scholten, Rev. Sci. Instrum. 75 (9) (2004) 3077.
[21] D.A. King, M.G. Wells, Surf. Sci. 29 (2) (1972) 454.
[22] P. Kisliuk, J. Phys. Chem. Solids 3 (1–2) (1957) 95.
[23] O. Lytken, W. Lew, J.J.W. Harris, E.K. Vestergaard, J.M. Gottfried, C.T. Campbell, J. Am. Chem. Soc. 130 (31) (2008) 10247.
[24] J. Liu, M. Xu, T. Nordmeyer, F. Zaera, J. Phys. Chem. 99 (16) (1995) 6167.
[25] H. Steininger, S. Lehwald, H. Ibach, Surf. Sci. 123 (2–3) (1982) 264.
[26] M. Kinne, T. Fuhrmann, C.M. Whelan, J.F. Zhu, J. Pantforder, M. Probst, G. Held, R. Denecke, H.P. Steinruck, J. Chem. Phys. 117 (23) (2002) 10852.
[27] B. Poelsema, R.L. Palmer, G. Comsa, Surf. Sci. 136 (1) (1984) 1.
[28] M. Lynch, P. Hu, Surf. Sci. 458 (1–3) (2000) 1.
[29] C.J. Zhang, R.J. Baxter, P. Hu, A. Alavi, M.H. Lee, J. Chem. Phys. 115 (11) (2001) 5272.
[30] K. Bleakley, P. Hu, J. Am. Chem. Soc. 121 (33) (1999) 7644.
[31] B. Hammer, L.B. Hansen, J.K. Norskøv, Phys. Rev. B: Condens. Matter Mater. Phys. 59 (11) (1999) 7413.
[32] J.L. Falconer, R.J. Madix, J. Catal. 48 (1–3) (1977) 262.
[33] J.L. Taylor, W.H. Weinberg, Surf. Sci. 78 (2) (1978) 259.